Ultrasonic Atomic Force Microscope with Overtone Excitation of Cantilever

Jpn. J. Appl. Phys. Vol. 35 (1996) pp. 3787–3792
Part 1, No. 6B, June 1996

Ultrasonic Atomic Force Microscope with Overtone Excitation of Cantilever

Kazushi YAMANAKA and Shizuka NAKANO
Mechanical Engineering Laboratory, Namiki 1-2, Tsukuba, Ibaraki 305, Japan

(Received January 8, 1996; revised manuscript received March 4, 1996; accepted for publication March 7, 1996)

We propose a novel atomic force microscope (AFM) combined with ultrasonic frequency vibration of a cantilever excited at its support. This method enables both topography and elasticity imaging of stiff samples such as metals and ceramics, without a need for bonding a transducer to the sample. When the sample surface is contacted with a tip attached to the cantilever, the cantilever vibration mode is changed according to the sample properties. It is theoretically predicted that the amplitude and resonant frequency of vibration at higher-order modes are useful parameters for elasticity evaluation of stiff samples. A preliminary experimental verification of this principle is presented using a glass-fiber-reinforced plastic sample. Clear elastic contrast was successfully obtained using a soft cantilever only when it was vibrated at MHz frequency higher-order modes.

KEYWORDS: atomic force microscope, ultrasonic vibration, higher-order mode, cantilever, resonant frequency, metal, ceramics

1. Introduction

The detection of ultrasonic frequency vibration in atomic force microscopy (AFM)[1] has been proposed and demonstrated, in which a sample is vibrated at frequencies much higher than the first resonant frequency of the cantilever.[2–9] These ultrasonic methods are attractive in material characterization because they can be used to evaluate the elasticity of stiff samples and to detect subsurface defects,[4–6] which are not possible by the force curves[10] and force modulation mode[11,12] using a soft cantilever. Although the force modulation mode using a very stiff cantilever ($> 1000\,\mathrm{N/m}$) can be used to evaluate a stiff sample such as fiber-reinforced plastics,[12] such a stiff cantilever is usually not acceptable in the contact mode since it easily damages a soft sample.

However, the reported ultrasonic methods face serious problems in their application to large, heavy or irregularly shaped samples, because such samples cannot be sufficiently or uniformly vibrated by a usual ultrasonic vibrator. It is also difficult to apply the ultrasonic methods to samples in an ultraclean environment, because they are easily contaminated by bonding agents for the vibrator. Since such samples are very important for application in microelectronics, micromachines and biology, we propose an alternative method that solves the above problems by avoiding bonding of a transducer to the sample, while maintaining the advantages of ultrasonic vibration.[13] In the proposed method, the sample can simply be placed on a sample stage of AFM, without the need for any bonding. In this paper, we present theoretical considerations and a preliminary experimental verification using a glass-fiber-reinforced plastic sample.

2. Principle

The principle of the proposed method is illustrated in Fig. 1. Figure 1(a) shows a cantilever vibration mode in AFM at low frequencies. Since the cantilever is soft, stiff samples such as metals, inorganic materials and ceramics do not deform and hence the stiffness of the sample cannot be evaluated. In Fig. 1(b) we propose an ultrasonic AFM, where higher-order mode vibration is excited on the cantilever by applying a vibrating force to its support. In this case the sample is deformed according to its stiffness. At the same time, parameters of the cantilever vibration, such as the resonant frequencies of higher-order modes, as well as the vibration amplitude at resonant frequencies, vary depending on the stiffness of the sample (these points are detailed in §3). Consequently, the stiffness of the sample can be evaluated by monitoring the cantilever vibration.

Figure 2 shows an implementation developed using a contact-mode AFM. In addition to usual functions of AFM,[1] a high-frequency vibrator attached to the support of a cantilever is driven in the high-frequency range of 0.1 to 10 MHz. Resultant vibration of the cantilever is detected by a photodiode and processed by a lock-in amplifier. We employ two detection schemes, defined as linear and nonlinear schemes.[2,3] In the linear detection scheme, the high-frequency signal is measured by the lock-in amplifier. Here, analysis of the measurement result is fairly simple because a linear model can be used, as shown in §3. However, a high-frequency photodiode and electronics of at least up to 1 MHz are required.

In the nonlinear detection scheme, the high-frequency signal is amplitude-modulated by a low-frequency generator around 1 to 10 kHz. Instead of the high-frequency signal, the low-frequency signal is employed as the reference of the lock-in amplifier. The advantage of this scheme is that we can use commercial AFM, since we do not directly measure the high-frequency signal out of the electronic bandwidth of commercial AFM (DC $\sim$ less

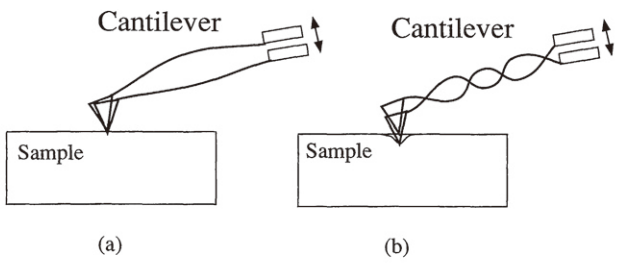

Fig. 1. Principle of the ultrasonic AFM enabling elastic imaging of large samples. (a) Vibration mode in AFM (Below the fundamental resonance) Sample does not deform and thus the elasticity cannot be evaluated, (b) Ultrasonic AFM (Higher-order mode vibration). Effective stiffness of cantilever is enhanced to deform the sample. Thus sample elasticity can be evaluated.

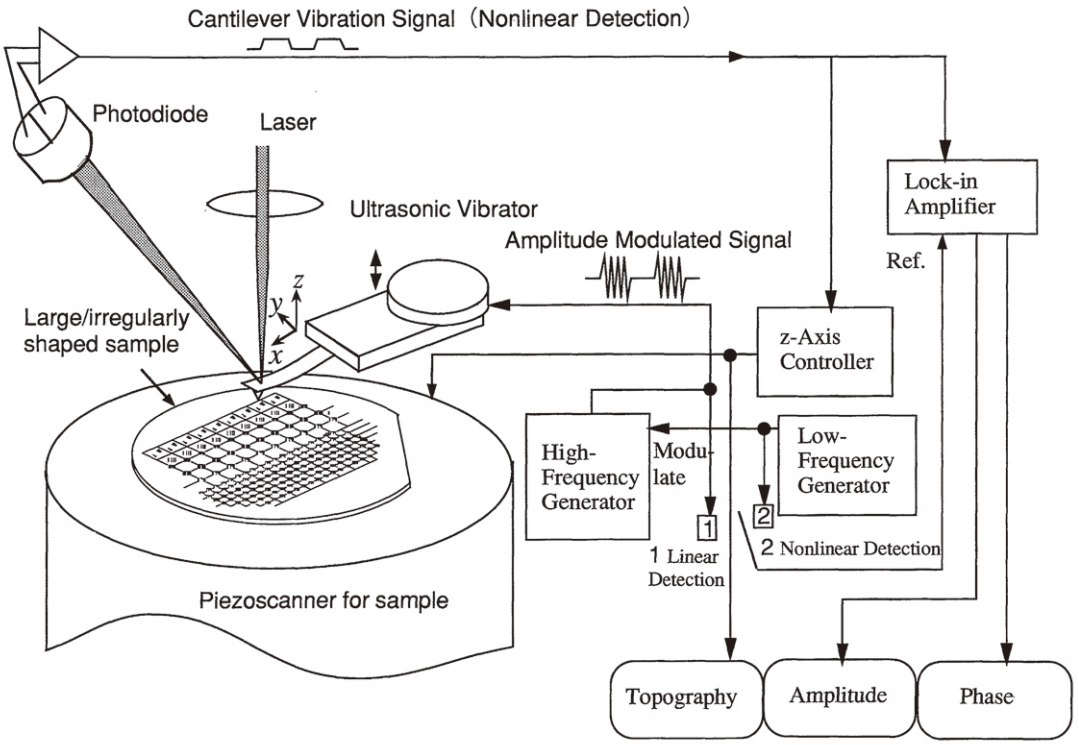

Fig. 2. Implementation of the principle with linear and nonlinear detection schemes.

than 200 kHz). Moreover, the use of the low-frequency signal is favorable for achieving a high signal to noise (S/N) ratio. However, the analysis is not so simple because the nonlinear tip-sample contact force must be considered to account for the generation of low-frequency vibration of the cantilever.

Since this method directly vibrates the cantilever, it is similar to the noncontact mode[14] and the tapping mode; however, the use of higher-order modes is unique to our method. Also, in contrast to the tapping mode, we can use very low amplitude vibration (< 0.1 nm) so that we can easily control the contact force to a very low level (< 0.1 nN). Finally, it is emphasized that there is no problem in the inspection of large samples (*e.g.*, VLSI wafers) and irregularly shaped samples (*e.g.*, turbine blades and magnetic recording heads), since transducer bonding to the sample is not required.

3. Analysis of Cantilever Vibration

3.1 *Resonant frequency*

In this section we show the advantages of employing higher-order modes. First, we show that the resonant frequency of higher-order modes is a useful parameter for stiffness evaluation of samples. For this purpose we calculated the resonant frequency of a cantilever by using an analytical model. The equation of two-dimensional (2D) deflection vibration of a cantilever in the x-z plane is given as

$$\frac{\partial^2 z}{\partial t^2} + \frac{Eh^2}{12\rho}\frac{\partial^4 z}{\partial x^4} = 0 \tag{1}$$

where E is Young's modulus, ρ is density and h is thickness of the cantilever.[15] The origin and x and z coordinates are taken as shown in Fig. 2. A solution of eq. (1) can be assumed to take the form of

$$z = C\sin(\omega t + \delta)\Phi(x) \tag{2}$$

with

$$\Phi(x) = (\sin\alpha + \sinh\alpha)\left(\cos\frac{\alpha}{L}x - \cosh\frac{\alpha}{L}x\right) + (\cos\alpha + \cosh\alpha)\left(\sin\frac{\alpha}{L}x - \sinh\frac{\alpha}{L}x\right), \tag{3}$$

where ω is the angular frequency, L is the length of cantilever and

$$\alpha = \left(\frac{12\rho\omega^2 L^4}{Eh^2}\right)^{\frac{1}{4}}. \tag{4}$$

The parameter α is determined from boundary conditions.[15,16] With solutions (2) and (3), the boundary condition for fixed cantilever at $x = 0$, i.e., $\Phi(0) = 0$ and $d\Phi(0)/dx = 0$, is always satisfied. If we further assume that the cantilever is supported at $x = L$ by a linear spring with stiffness s, the boundary condition is

$$F(L) = sz(L), \tag{5}$$

where $F = \partial M/\partial x$ is the force and $M = (Ewh^3/12)(\partial^2 z/\partial x^2)$ is the bending moment[15] where w is the width of the cantilever. From eqs. (2) and (5) we obtain

$$\frac{k}{3}\frac{\partial^3\Phi}{\partial x^3}(L) = s\Phi(L), \tag{6}$$

where $k = Ew/4(h/L)^3$ is the stiffness (spring constant) of the cantilever. Substituting eq. (3) into eq. (6), we obtain the frequency equation

$$\frac{k}{3s}\alpha^3 P(\alpha) = Q(\alpha), \tag{7}$$

where $P(\alpha)$ and $Q(\alpha)$ are defined as

$$P(\alpha) = 1 + \cos\alpha \cosh\alpha,$$
$$Q(\alpha) = \cos\alpha \sinh\alpha - \sin\alpha \cosh\alpha. \quad (8)$$

Once eq. (7) is solved for α, the resonant frequency is obtained using eq. (4). For a very stiff sample ($s \gg k$), eq. (7) approaches $Q(\alpha) = 0$, which is the frequency equation of a supported cantilever, derived from the boundary condition $\Phi(L) = 0$ and $\Phi''(L) = 0$. Alternatively, for a very soft sample ($s \ll k$), eq. (7) approaches $P(\alpha) = 0$, which is the frequency equation of a free cantilever derived from the boundary conditions $\Phi''(L) = 0$ and $\Phi'''(L) = 0$.[15,16]

Equation (7) was numerically solved, assuming a typical silicon nitride cantilever with $E = 144\,\mathrm{GPa}$, $\rho = 3.15 \times 10^3\,\mathrm{kg/m^3}$, $h = 0.8\,\mu\mathrm{m}$ and $L = 200\,\mu\mathrm{m}$. The resonant frequencies of the first ($n = 1$) through the fifth ($n = 5$) modes are plotted in Fig. 3 as a function of the stiffness ratio γ defined as k/s in the range of 10^{-5} and 10^2.

It is noted that the resonant frequency decreases as γ increases only in a limited range. The most important finding is that this range differs among different modes. For example, the resonant frequency of the first mode ($n = 1$) remains constant at a value similar value to that of a supported cantilever in the range of γ less than 10^{-2}. The resonant frequency of the first mode shows substantial decrease in the range of 10^{-2} to 10^0, following the decrease in stiffness of the sample, and then reaches an almost constant value of a free cantilever in the range above 10^0. On the other hand, the resonant frequency of the fourth mode ($n = 4$) remains almost constant in the range less than 10^{-4}, shows substantial decrease in the range of 10^{-4} to 10^{-2}, and then reaches an almost constant value above 10^{-2}.

Consequently, the resonant frequency of the first mode is useful for characterizing soft samples ($\gamma = 10^{-2}$ to 10^0), whereas those of the higher-order modes are suitable for stiff samples ($\gamma = 10^{-4}$ to 10^{-2}). Therefore we want to stress that complementary use of higher-order modes in addition to lower-order modes enables, for the first time, stiffness evaluation of a wide range of materials from, for example, ceramics to organic molecules.

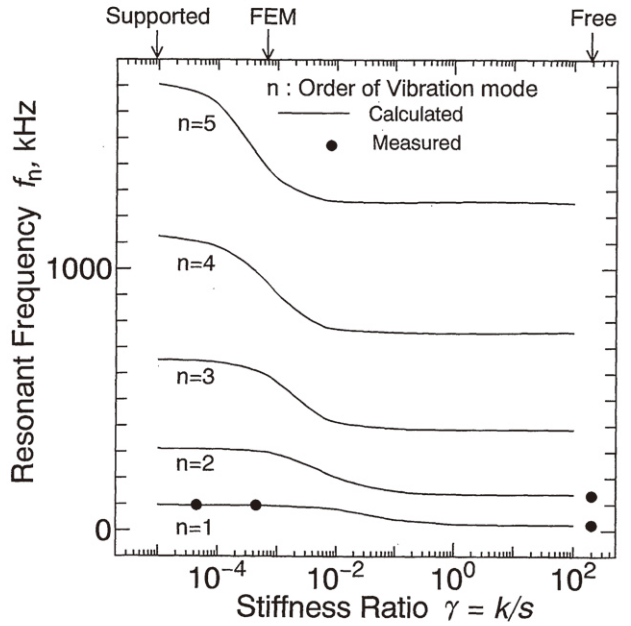

Fig. 3. Relationship between cantilever resonant frequency and stiffness of sample. The stiffness of sample is normalized by cantilever stiffness k.

3.2 *Deformation of sample*

Next, we show that a stiff sample can be deformed even when a soft cantilever is vibrated at higher-order modes, although the sample is not deformed at lower-order modes. Since the stiffness of the sample can be evaluated by measuring the cantilever vibration when the sample is deformed, this point is important for establishing the principle of our method.

For this purpose the vibration mode of the cantilever was analyzed using three-dimensional (3D) finite-element analysis method (FEM).[17] We assumed that the width of the cantilever w is 20 μm, Poissons ratio is 0.248, and other parameters are identical with those for the 2D cantilever described in §3.1, which resulted in the cantilever stiffness k of 0.045 N/m. The boundary condition was also that one end was fixed and the other end was supported by a spring representing the tip-sample contact stiffness. The spring was simulated by a rectangular

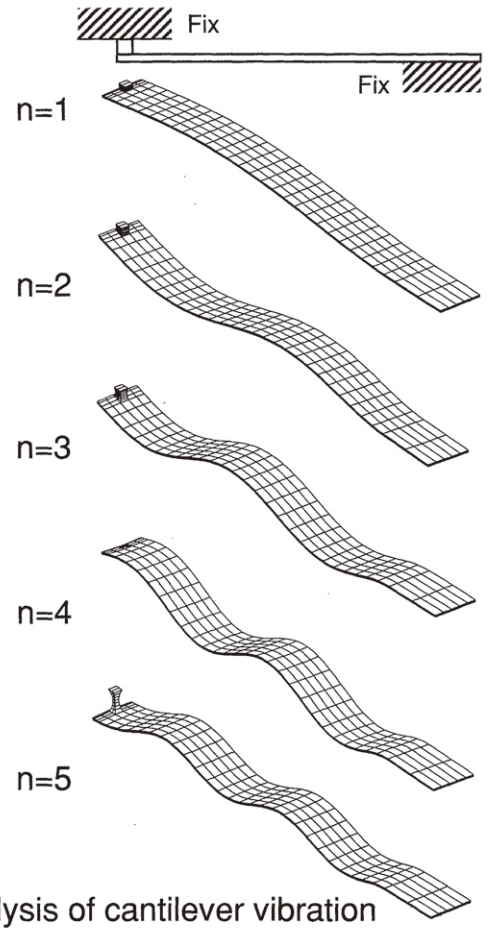

Fig. 4. First- and higher-order vibration modes of a cantilever fixed at one end (right side) and supported by a spring (left side). The spring is simulated by a rectangular column of elastic material whose top surface is fixed.

column ($4 \times 4 \times 2.8\,\mu$m) of elastic material located on the upper face of the left edge of the cantilever, as shown at the top of Fig. 4. Deformation of this rectangular column represents the deformation of the sample induced by the tip. The Young's modulus of 12.5 MPa, Poisson's ratio of 0.248 and density of 3.15×10^3 kg/m^3 were assumed for this column, which resulted in the tip-sample contact stiffness s of 53.3 N/m. For this cantilever and contact stiffness, the stiffness ratio γ is 8.4×10^{-4}, satisfying the condition of a soft cantilever, $s \gg k$.

As a result of eigenvalue analysis, vibration modes of $n = 1$ to 5 are illustrated in Fig. 4, where n represents the order of the vibration mode. It is clearly seen that the rectangular column representing stiffness of the sample negligibly deforms in modes of $n = 1$ and 2. Consequently, a small variation in the sample stiffness would not bring a significant difference in the cantilever vibration amplitude. On the other hand, the sample is significantly compressed in the mode of $n = 4$, and is stretched in the mode of $n = 5$. In this situation, a small variation in the sample stiffness is expected to change the magnitude of sample deformation. At the same time, this variation changes the cantilever vibration amplitude, and this change, in turn, can be detected by the laser probe.

In other words, a cantilever softer than the tip-sample contact stiffness is effectively stiffened in the higher-order mode, and can be used to evaluate the sample elastic property. The reason for this stiffening may be explained by the inertia of the cantilever/tip as well as the formation of a node along the cantilever axis. The distance between the tip and the closest node is much less than the original cantilever length, resulting in effective shortening of the cantilever.

4. Images of Fiber Composite

In this section we show the advantages of the ultrasonic AFM by applying it to a glass-fiber-reinforced plastic (PEEK; polyether ether ketone) sample. We assume that the effective elasticity E^* (determined from Young's modulus and Poisson's ratio) of the glass and PEEK is 50 GPa and 5 GPa, respectively, and that the contact radius A is 10 nm for both. Then the contact stiffness s, evaluated as $2E^*A$,[18] is 1000 N/m and 100 N/m, respectively. This sample was imaged using a cantilever with stiffness k of 0.045 N/m identical to those described in §3 for 3D FEM calculation. The stiffness ratio γ is then 4.5×10^{-5} and 4.5×10^{-4} for the glass and PEEK, respectively.

The cantilever support was vibrated using a PZT bimorph transducer in the frequency range between 1 kHz and 2 MHz. In the linear detection scheme, the first resonant frequency of the free cantilever was observed at 22.2 kHz and the second at 133.7 kHz. When the tip contacted either the PEEK resin or the glass fiber at a contact force of 1 nN, the first resonant frequency increased to 96.9 kHz. Clearly the two materials could not be distinguished on the basis of the first resonant frequency. These measured frequencies are plotted in Fig. 3 against the stiffness ratio, and agree with the calculated frequency curves for $n = 1$ and $n = 2$. The resonant frequency of higher-order modes was above 200 kHz and could not be detected in the present electronic bandwidth, and hence detailed verification of the resonant frequency characteristics predicted in Fig. 3 is left for future study.

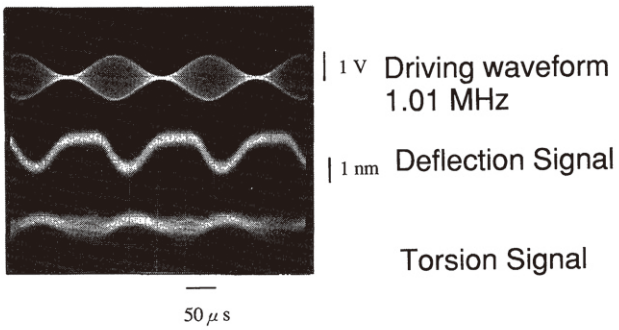

Fig. 5. Observed signals. Top trace: amplitude-modulated high-frequency signal for driving the ultrasonic vibrator attached to the cantilever support, Middle trace: Cantilever deflection signal, Bottom trace: Cantilever torsion signal.

We applied the nonlinear detection scheme at frequencies above 200 kHz in the present work. We vibrated the cantilever support using a high-frequency signal at 1.01 MHz, the fourth resonant frequency of the cantilever, whose amplitude was modulated by a low-frequency signal at 6 kHz as shown by the top trace in Fig. 5. Then the cantilever deflection vibration at the modulation frequency was observed as shown by the middle trace in Fig. 5. The down-going signal represents the upward deflection of the cantilever. The upper half of the waveform shows a plateau rather than a sine wave. This plateau indicates that the nonlinear response is very small when the vibration amplitude is less than a certain threshold, as described in previous communications.[3-5]

The cantilever torsion vibration was also slightly excited as a result of crosstalk from deflection, as shown by the bottom trace of Fig. 5, although this crosstalk is negligible compared to the deflection. This is an important characteristic for precise measurement of elasticity, since the existence of the crosstalk indicates that the direction of the tip sample contact force is not perfectly aligned along the z direction.

Figure 6(a) shows a topography image of a $20 \times 20\,\mu$m area, with the maximum height difference of 1316 nm. Although a glass fiber of about 5 μm diameter partially buried in the PEEK matrix was clearly identified, material discrimination between the glass and PEEK was not possible. However, clear contrast was obtained in the ultrasonic image between the components, as shown in Fig. 6(b). Figure 7 is a magnified view of Fig. 6 including a boundary region between glass and PEEK. It was found that the upper right side of the glass fiber is covered with a 10 to 20-nm-thick layer of some material, from careful examination of the topography image in Fig. 7(a). Correspondingly, the ultrasonic image in Fig. 7(b) of the layered area shows brightness between brightnesses on the glass fiber and on the PEEK. This observation suggests that the layer consists of the PEEK, adhered to the glass fiber, probably showing a good affinity between the glass fiber and the PEEK. Thus it is ex-

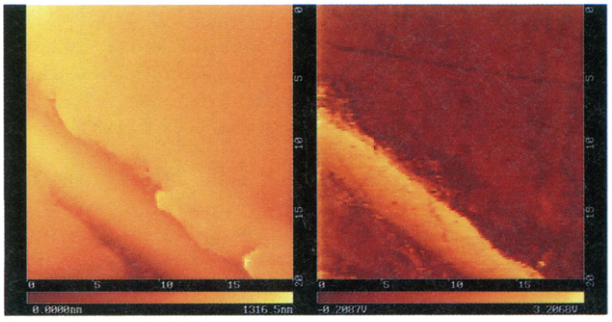

(a) (b)

Fig. 6. Images of a glass-fiber-reinforced plastic (PEEK). (a) Topography, (b) Ultrasonic image by nonlinear detection. High frequency: 1.01 MHz, Amplitude modulation: 6 kHz

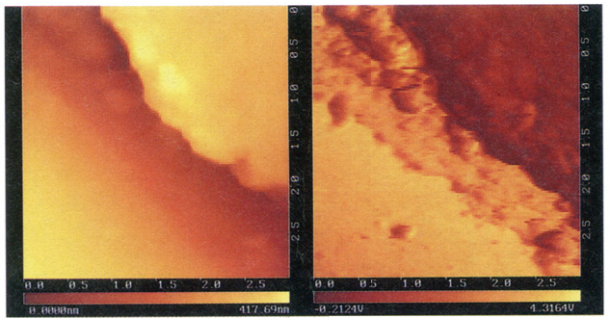

(a) (b)

Fig. 7. Magnified view of Fig. 6 including the boundary region of glass and plastic. (a) Topography, (b) Ultrasonic image by nonlinear detection. High frequency: 1.01 MHz, Amplitude modulation: 6 kHz

pected that the ultrasonic AFM can evaluate the stiffness of a thin layer on the order of a few tens of nanometers.

Finally we make a brief comparison with the conventional low-frequency force modulation image of the identical area taken at a modulation frequency of 6 kHz, as shown in Fig. 8. Figure 8(a) is obtained by vibrating the cantilever, whereas Fig. 8(b) is obtained by vibrating the sample. In contrast to the ultrasonic images, it is difficult to distinguish the glass from the PEEK, since the brightness change in the two areas is very small, as expected from the analysis described in §3. Another interesting point is that two scratches were observed at an abrupt height variation near the boundary between glass fiber and PEEK, which were not observed in the ultrasonic images. Another advantage of the ultrasonic AFM is that it is relatively free from such scratches, though at present we do not know the reason for it.

5. Conclusions

We proposed and verified a novel AFM that can discriminate elasticity of stiff samples. The advantage of the present method over the previous AFM using ultrasonic vibration is that bonding a transducer to the sample is not needed, and limitations of the size and shape of the sample are eliminated. Problems due to contamination by bonding agents are also avoided. It was shown for the

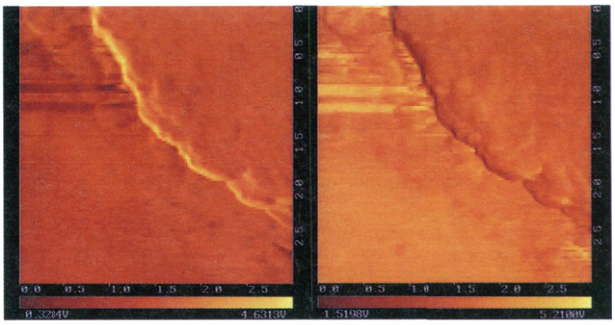

(a) (b)

Fig. 8. Force modulation images at 6 kHz. (a) Cantilever vibration method, (b) Sample vibration method.

first time that the higher-order modes play a complementary role to the lower-order modes in the evaluation of a wide range of materials. As an example of possible application of this unique feature, the elasticity of the interfacial area of biological macromolecules and the microstructure of ceramic implants could be investigated. Although the elasticity of macromolecules and ceramics differ by orders of magnitude, it is possible to evaluate both by complementary use of lower- and higher- order mode vibrations (see Fig. 3). Such a measurement could provide important information on the affinity of an implant material to biological tissues.

Although the present experiment was mostly restricted to the nonlinear detection scheme, linear detection will be fully realized either by using a cantilever of lower resonant frequency or by improving the high-frequency bandwidth of the detection electronics. Furthermore, another nonlinear detection scheme by frequency mixing is also worth investigating, in which a vibration is applied to the sample with a frequency slightly different from that of the cantilever support and the cantilever vibration is detected with a frequency equal to the difference between the frequencies of the sample and the cantilever support. Advantages of this scheme are that the vibration amplitude can be kept constant, and that the phase measurement is easier than in the amplitude modulation method.

1) G. Binnig, C. F. Quate and Ch. Gerber: Phys. Rev. Lett. **56** (1986) 930.
2) W. Rohrbeck and E. Chilla : Phys. Status Solidi (a) **131** (1992) 69.
3) O. Kolosov and K. Yamanaka: Jpn. J. Appl. Phys. **32** (1993) L1095.
4) K. Yamanaka, H. Ogiso and O. Kolosov: Appl. Phys. Lett. **64** (1994) 178.
5) K. Yamanaka, H. Ogiso and O. Kolosov: Jpn. J. Appl. Phys. **33** (1994) 3197.
6) K. Yamanaka: Thin Sol. Films **273** (1996) 116.
7) U. Rabe and W. Arnold: Appl. Phys. Lett. **64** (1994) 1493.
8) U. Rabe and W. Arnold: Ann. Phys. **3** (1994) 589.
9) N. A. Burnham, A. J. Kulik, G. Gremaud, P.-J. Gallo and F. Oulevey: Abst. Eighth Conf. Scanning Tunneling Microscopy, Snowmass, 1995.
10) M. Heuberger, G. Dietler and L. Schlapbach: Nanotechnology **5** (1994) 12.
11) M. Radmacher, R. W. Tillmann and H. E. Gaub: Biophys. J.

64 (1993) 735.
12) P. Maivald, H. J. Butt, S. A. C. Gould, C. B. Prater, B. Drake, J. A. Gurley, V. B. Elings and P. K. Hansma: Nanotechnology **2** (1991) 103.
13) K. Yamanaka and S. Nakano: Abst. Third Int. Colloq. Scanning Tunneling Microscopy, Kanazawa, (1995) p. 59.
14) Y. Martin, C. C. Williams and H. K. Wickramasinghe: J. Appl. Phys. **61** (1987) 4723.
15) for example; K. Nakagawa, Y. Murotsu and T. Iwatsubo: Kougyou Sindou Gaku (Engineering Vibration Mechanics) (Morikita, Tokyo, 1976). [in Japan]
16) H-J. Butt and M. Jaschke: Nanotechnology **6** (1995) 1.
17) *Piezo Plus*, Dynus Inc. Japan.
18) W. C. Oliver and G. M. Pharr: J. Mater. Res. **7** (1992) 1564.